Arch. Metall. Mater. **70** (2025), 1, 127-134

DOI: https://doi.org/10.24425/amm.2025.152526

M. RADHIKA[1,2*], ANJANEYA PRASAD. B.[1], SURESH AKELLA[3]

COMPARISON OF THE PERFORMANCE OF GROUNDNUT SHELL-BASED CARBON-REINFORCED PLA COMPOSITES, FABRICATED USING INJECTION MOLDING AND PELLET 3D PRINTING

This study intended to investigate the impact of two distinct shaping methods, Injection molding and pellet additive manufacturing, on tensile and thermal properties of PLA based materials. It included comparisons of neat PLA and PLA reinforced with carbon nanoparticles derived from groundnut shells (GNSC) via pyrolysis at 800°C. These nanoparticles were characterized using FTIR, XRD, FESEM, and EDX analyses to assess their carbon content, morphology, and structure. The synthesized carbon was used as a reinforcement filler in the PLA matrix and biobased polymer nanocomposites were prepared by pellet 3D printing and injection molding. The mechanical and thermal characteristics of PLA/GNSC composite specimens with 0.25, 0.5, and 0.75 wt% of GNSC nanoparticles were compared. Reinforcing PLA with GNSC nanoparticles improved tensile properties in both shaping techniques. The PLA/GNSC_0.5 exhibited the greatest tensile strength, measuring 58.61 MPa for injection molded samples and 53.05 MPa for 3D printed samples, representing a 50% enhancement compared with neat PLA. The tensile modulus was also highest for PLA/GNSC_0.5, measuring 1.24 GPa for injection molded samples and 1.21 GPa for 3D printed samples, representing an improvement of 14% compared with neat PLA. The tensile characteristics showed a modest increase in tensile strength (9-13%) and a slight improvement in tensile modulus (2-3%) for injection molded samples compared to 3D printed samples. The thermal properties showed no substantial variation between the two shaping methods. These findings highlight the effectiveness of GNSC nanoparticles in enhancing the mechanical and thermal performance of PLA composites, regardless of the shaping technique.

Keywords: PLA; Pellet 3D printing; Injection molding; Ground nut shell; biocarbon

1. Introduction

In light of the global limitation of petroleum resources, there has been a notable upsurge in interest in non-petroleum-based polymers in both industrial and scientific domains. Biopolymers are polymers sourced from renewable biological origins, including plants, animals, algae, or microorganisms [1]. Biopolymers are biodegradable, undergoing natural decomposition facilitated by microorganisms. These microorganisms break down the polymer components into simpler compounds through enzymatic processes, causing no harm to the environment [2]. These materials have garnered considerable attention owing to their capacity to tackle environmental issues linked with conventional polymers derived from fossil fuels. The biopolymers offer several environmental advantages, including reduced carbon footprint, biodegradability, and potential for renewable sourcing [2].

PLA is the most impactful biopolymer derived from renewable resources like corn, potato starch, and sugar cane molasses through fermentation and subsequent ring-opening polymerization processes. PLA has high tensile strength, high stiffness, excellent processability coupled with renewable nature, biodegradability, and relatively high availability [3-4]. While PLA boasts numerous advantages, it also presents several drawbacks including limited flexibility, inherent brittleness and low toughness, a relatively low service temperature, and inadequate melt strength. These drawbacks are overcome by modifying PLA with fillers, and plasticizers and blending with another polymer [5]. The addition of nanofillers is a highly successful approach to overcome the limitations of biopolymers and create products with customized features for a broader range of applications [6]. Nanofillers are characterized by at least one dimension that falls under the nanometre scale, usually less than 100 nanometres. Their exceptionally high surface-to-volume ratio fundamentally changes the properties of a polymer in comparison to larger-scale fillers. Through precise control of particle size, interactions with the polymer, and dispersion within the matrix, incorporating a very little loading percentage of nanofillers (typically less than 10 wt%) has shown remarkable potential to modify material

[1] JAWAHARLAL TECHNOLOGICAL UNIVERSITY HYDERABAD, TELANGANA, INDIA
[2] VIGNAN INSTITUTE OF TECHNOLOGY AND SCIENCE, DESHMUKHI, HYDERABAD, TELANGANA, INDIA
[3] SREYAS INSTITUTE OF ENGINEERING AND TECHNOLOGY, NADERAGUL, HYDERABAD, TELANGANA, INDIA
* Corresponding author: mandalaradhika77@gmail.com

properties significantly. This includes improvements in strength, stiffness, toughness, thermal resistance, and barrier properties. Additionally, it also enhances the melt strength and retards the crystallization process of PLA. Currently, a range of nanofillers is utilized to strengthen PLA-based composites, including layered nano silicates, nano silica, single-wall and multi-wall carbon nanotubes [7], graphene [8-10], silver, and titanium dioxide [11,12]. However, these nanofillers are derived from fossil fuel, and producing nanoparticles often requires sophisticated and energy-intensive processes which can contribute to higher production costs and environmental impacts. In addition, it is important to note that these nanofillers are not capable of undergoing natural decomposition or being derived from biological sources. The inclusion of non-biodegradable fillers in environmentally-friendly polymers compromises the sustainability of the material and adds complexity to the procedures of recycling or composting.

Therefore, it is crucial to prioritize the creation of bio-based carbon nanofillers that are sustainable, renewable, and degradable to produce "green composites" or "biocomposites" based on PLA [4]. Various natural fillers like sugarcane bagasse, rice husk, groundnut shell powder, and wood flour particles have been used for reinforcement for producing green composites [13,14]. However, their inherent hygroscopic nature poses challenges, potentially causing dimensional changes, decreased mechanical properties, and heightened susceptibility to degradation in humid or wet environments. Rather than directly adding natural fillers, reinforcements such as cellulose, lignin, chitosan, and biochar derived from natural sources can be effectively utilized for enhancing composite materials[10].

The utilization of biochar or biocarbon in making biocomposites has garnered global scientific interest and has been recognized as a potential filler due to its low density, high strength-to-weight ratio, high thermal stability, and low cost [15]. Biochar is synthesized by pyrolysis using a various biomass precursor, such as agro-waste, industrial residue, forestry residue, and municipal solid waste. The synthesized biochar was reinforced as a filler material for making PLA/biochar composites. Ertane et al. [16] developed a 3D printable filament for 3D printing combining wheat stem-derived biochar with PLA. The study aimed to assess the wear behaviour of the composite. Results showed enhanced wear resistance with biocarbon addition, notably at 30 vol%. However, higher biocarbon volumes correlated with increased nozzle clogging. In their study, Huang et al. [17] found that incorporating grapevine biochar into PLA resulted in substantial enhancements in both the tensile and impact strengths of the composite. Specifically, the tensile strength increased by 41.4%, and the impact strength improved by 32.1% compared to pure PLA. Pudełko et al. [18] noted an improvement in the thermo-mechanical properties of composites through the incorporation of biochar synthesized from sewage sludge into the PLA matrix. The flame retardance properties also improved with the inclusion of biochar derived from miscanthus and wood chips into PLA. Aup-Ngeon et al. [19] synthesized biocarbon from various agro-waste and reinforced with PLA. The PLA composite, featuring a 25 wt% loading of biochar, demonstrated a notable 21% increase in tensile modulus and a substantial 76% increase in impact strength. It's worth noting that these micro-sized particles necessitate a higher loading percentage to improve properties due to their lower surface area to volume ratio. The nano-sized particles have a higher surface-to-volume ratio which requires lower wt% of loading. In a study of Umerah et al. [20], a 3D printable filament was created by incorporating carbon nanoparticles derived from coconut shells into PLA/ Bioplast. The addition of carbon nanoparticles at lower weight percentages (0.2 wt% and 0.6 wt%) led to improved mechanical and thermal properties compared to neat bioplast. However, at higher loadings of carbon nanoparticles, properties decreased due to agglomeration issues. Mei-po Ho et al. [21] prepared a PLA/bamboo biochar composite with a loading of 2 to 10 wt%. For 7.5 wt% loading the maximum tensile strength of the composite was 43% higher than neat PLA. For further increasing the filler content the tensile strength was decreased.

Groundnut shells, also known as peanut shells or hulls, are the outer covering of groundnut seeds. They are a byproduct of the agricultural processing of peanuts, typically discarded after the seeds are extracted for oil production or direct consumption [22]. It consists of 44% cellulose, 36% lignin and 6% hemicellulose are efficiently used to produce carbon nanoparticles. Biocarbon derived from groundnut shell can be effectively used as a reinforcement filler in making biobased polymer nanocomposites [23]. Groundnut shells are abundantly available agro-waste in India as it is the second largest country in producing groundnut. Hence, in this study the groundnut shells were used to produce carbon nanoparticles.

PLA and biocarbon can be molded using conventional methods like injection molding. However, a significant drawback of these traditional molding procedures is their requirement for a substantial initial investment in equipment and tools. Consequently, these methods are only feasible for large-scale mass production. 3D printing is now seen as a viable substitute for producing small batches [14]. Franchetti et al. [24] conducted a cost analysis comparing injection molding and 3D printing for different batch sizes. They identified "break-even points" where injection molding becomes cost-effective. The study concluded that injection molding is more economical and faster for high-volume production, while 3D printing is only viable for small-batch production. The tensile properties of pure acrylonitrile butadiene styrene (ABS) and specimens of its nanocomposite, containing 1, 3, and 5 weight percent montmorillonite (MMT), were compared by Weng et al. [25]. Two shaping techniques injection molding and fused deposition modeling (FDM) were used to fabricate the specimens. It was identified that the tensile characteristics of the FDM samples were inferior to those of the injection-molded ones. However, by selecting optimum process parameters the mechanical and thermal characteristics can be improved. In Miller et al.'s [26] work, thermoplastic polycarbonate urethane (PCU) samples were fabricated utilizing injection molding and FDM to assess and compare the mechanical characteristics of the samples. Through the utilization of appropriate printing parameters and the exceptional durability of PCU, the

3D-printed samples exhibited mechanical properties that were equivalent to those of the injection-molded samples. Kayank et al. [27] also compared the mechanical performance of PLA, PLA reinforced with glass fibre and PLA blended with thermoplastic polyurethane elastomer (TPU) produced using fused deposition modeling and injection molding. There is no significant difference in mechanical characteristics of injection molded and 3D printed samples for neat and blended PLA. Nevertheless, the tensile strength and tensile modulus of glass fibre reinforced PLA samples produced by FDM are reduced by 32% and 41% compared to injection molded specimens. The thermal degradation values of the samples remained similar regardless of the molding technique. The 3D printed specimens exhibited greater crystallinity in comparison to those produced using injection molding. Komal et al. [28] analyzed to compare the performance of parts produced using FDM versus injection molding in terms of their thermal, mechanical, and crystallographic properties. At the optimal combination of process parameters, 3D-printed specimens surpass injection-molded specimens.

The commercial feasibility of biocomposites relies on the production technique that offers reduced processing time, operational simplicity, outstanding dimensional qualities, and reproducibility. Hence, it is aimed to compare, for the first time, the impact of two shaping techniques pellet additive manufacturing and injection molding on the mechanical and thermal performance of neat PLA and PLA reinforced with groundnut shell derived carbon nanoparticles (GNSC). The carbon nanoparticles derived from groundnut shell powder pyrolyzed at 800°C in a tube furnace. The synthesized nano particles in various weight % (0.25, 0.5, and 0.75 wt%) is used as a reinforcement in the preparation of PLA/GNSC composites. The PLA/GNSC composite samples were produced using two different shaping methods: 3D printing and injection molding. The mechanical and thermal properties of these samples were evaluated in order to determine the impact of the shaping procedure.

2. Experimental

2.1. Raw materials

Groundnut shells are collected from the local farmers in Hyderabad, India. Clear Polylactic acid (PLA) in pellet form (TC175 Grade), with a melt flow index of 3 g/10 min, was sourced by 2M BIOTEC LLP, Tamil Nadu, India. Chloroform ($CHCl_3$, ≥99%) was procured from Lab Tech Corporation in Hyderabad, Telangana, India, and employed for dissolving the PLA.

2.2. Methods

2.2.1. Preparation of Groundnut shell powder (GNSP)

The harvested groundnut shells underwent a cleaning process with water to remove dirt, followed by sun-drying for three days. Subsequently, they were dehydrated in a hot air oven at 80°C for 48 hours to eliminate residual moisture. Once dried, the groundnut shells were finely ground using a kitchen mixer and sifted with a laboratory sieving machine to achieve uniform particle size of 60 μm. The resulting groundnut shell powder, labeled as GNSP, was stored in an airtight container.

2.2.2. Synthesis of carbon nanoparticles

The prepared GNSP was taken (5 g) into a silica crucible and kept in the tube furnace for the pyrolysis process. The tube furnace was heated to 800°C at a ramping rate of 10°C per minute. The pyrolysis of GNSP took place under an inert atmosphere of nitrogen gas, with a flow rate of 150 ml/cm^3. The GNSP was held at this temperature for 1 hour, after which it was cooled to room temperature at a rate of 2°C per minute. The carbon samples obtained from groundnut shells are labeled as GNSC800.

2.2.3. Preparation of biobased polymer nanocomposite

The synthesized GNSC800 was dispersed in chloroform (1:100 weight/volume) at concentrations of 0.25, 0.5, and 0.75 wt% using ultrasonication for 3 hrs. The PLA pellets were dissolved in chloroform at a ratio of 1:5 (weight/volume) with continuous magnetic stirring for 3-4 hours. The GNSC800/chloroform solution and PLA/chloroform solution were combined and stirred continuously using a magnetic stirrer for the whole night, resulting in the formation of a PLA/GNSC800 solution. The slurry is deposited onto a glass plate and allowed to desiccate overnight. During the drying process, chloroform evaporates and the suspension changes into a thin layer. The dried thin layer separates off the glass plate and is subsequently divided into small fragments. The diced fragments were subjected to thermal treatment in a high-temperature hot air oven maintained at 80°C for a duration of 3 to 4 days.

2.2.4. Injection moulding

A vertical plunger injection molding machine (Texair Plastic Machinery, INDIA) having a 3mm nozzle diameter was used for creating tensile test specimens by using aluminium molds. The mold was designed according to ASTM D638 Type-IV. PLA/GNSC pellets were introduced into the feed hopper, and the mold temperature was adjusted to 45°C. The samples prepared by injection moulding are labeled as IM_PLA, IM_PLA/GNSC_0.25, IM_PLA/GNSC_0.5 and IM_PLA/GNSC_0.75.

2.2.5. 3D printing with pellet extruder

Tensile test samples were fabricated from the PLA/GNSC pellets using Garuda3D, DP500 pellet extruder as depicted in

Fig. 1. The prepared PLA/GNSC pellets were introduced into the hopper of the pellet extruder. An auger, which serves as a feeding device, transfers the pellets from the hopper to the nozzle. The printer's nozzle was maintained at a temperature of 200°C. The temperature is precisely controlled to the point where the pellets undergo a phase shift and become molten. The liquefied substance is propelled through a nozzle of 1mm diameter onto the print bed. TABLE 1 provides the printer settings and process parameters. Tensile test specimens were printed as per ASTM standard D638 Type-IV. The printed samples labeled as3D_PLA, 3D_PLA/GNSC_0.25, 3D_PLA/GNSC_0.5 and 3D_PLA/GNSC_0.75.

Fig. 1. Pellet 3D printer

TABLE 1

Printer settings and Process parameters

Parameter	Values
Nozzle diameter	1mm
Printing speed	25mm/sec
Extrusion temperature	200°C
Model	Garuda3d, DP500
Machine dimensions	500 × 500 mm
Power	150 Watt
tolerance	±0.5%
Layer height	0.25 mm
Infill density	100%
Infill orientation	45 degree

2.3. Material characterization

2.3.1. Carbon nanoparticles characterization

The Perkin Elmer equipment was used to acquire the Fourier transform infrared spectrum (FTIR), which spanned a range from 4000 to 400 cm^{-1}. The objective of this research was to determine the functional groups contained in the sample and to confirm the complete carbonisation of groundnut shell powder. The Fourier transform infrared spectrum (FTIR) was acquired using a Perkin Elmer instrument, covering a range from 4000 to 400 cm^{-1}. This analysis aimed to identify the functional groups present in the material and to confirm the complete carbonization of groundnut shell powder. The microstructure of the carbon nanoparticles produced during pyrolysis was examined using Field Emission Scanning Electron Microscopy (FESEM) with an acceleration voltage of 15 kV, employing a JEOL JSM-7100F instrument. The size of the nanoparticles was determined using ImageJ software. The elemental composition of GNSC800 was determined via Energy-dispersive X-ray spectroscopy (EDX). X-ray diffraction (XRD) analysis was conducted using a PAN analytical X-ray diffractometer in the 2θ range of 10°-90° to analyze the phase composition of the material.

2.3.2. Characterization of GNSC/PLA composite

2.3.2.1. Thermogravimetric (TGA) analysis

Thermal behaviour of PLA/GNSC composite analyzed by conducting thermogravimetric analysis using TGA instrument of model TGA: 4000. The PLA and PLA/GNSC composite of both injection molded and 3D printed specimens were heated at a rate of 10°C/min from 30°C to 800°C under a nitrogen environment.

2.3.2.2. Tensile testing

The tensile characteristics of the 3D printed specimens were determined using a UTES40 HGFL universal testing equipment (Fuel Instruments & Engineers, INDIA). Fig. 2 displays the CAD model of the tensile test specimen (ASTM D638 Type-IV). The tensile modulus was calculated from the slope of the linear portion of the acquired stress-strain curves using Origin software. The data shown represents the mean value obtained from conducting five tests on each specimen for every property assessed.

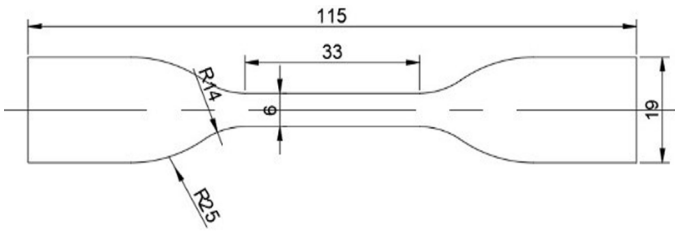

Fig. 2. Tensile test specimen as per ASTM D638 Type-IV

3. Results and discussion

3.1. Characterization of GNSC particles

FTIR spectra of groundnut shell powder and pyrolyzed carbon nanoparticles are presented in Fig. 3. The broad peak observed around 3323.8 cm^{-1} in the GNSP spectrum corresponds to the stretching of O-H bonds, while the peak around 2914.28 cm^{-1} is attributed to the stretching of C-H bonds [29,30]. The presence of a peak at 1604.7 cm^{-1} can be attributed to the stretching of

the C-O bond. Additionally, the peak observed at 1026.19 cm^{-1} is attributed to the presence of cellulose and hemicellulose, specifically the stretching of C-O-H bonds [31]. However, upon examining pyrolyzed GNSC800, it is evident that there were no notable peaks in the spectra. This indicates that the groundnut shell powder has completely pyrolyzed and the surface functions of carbon have been eliminated, resulting in a rather inert state. Consequently, when the temperature increases, the biochar undergoes substantial carbonization, leading to the formation of graphite-like structures [32].

In the XRD graph (Fig. 4), the peaks observed between 2θ = 18°-30° correspond to the stacked arrangement of aromatic layers, specifically indicating the graphite (002) orientation. Additionally, the peak at 2θ = 43°, conforming to the (101) plane, suggests the presence of graphitic content [31]. At 24° there is a broad peak which indicates the amorphous nature of synthesized carbon. Additionally, there are sharp peaks at 26° and 29° that show the presence of a crystalline arrangement. From this it can be concluded that the carbon produced exhibits a semi-crystalline structure. Other unlabelled peaks likely indicate the presence of inorganic compounds within the sample. The morphology of the carbon nanoparticles derived from the pyrolysis of groundnut shell powder at a temperature of 800°C is depicted in Fig. 5. The SEM micrographs confirm that the carbon particles generated at this temperature are of nanoscale dimensions and possess a spherical shape. The histogram illustrates that the all most all of particles are concentrated within the size range of 10-40 nm. The EDX spectrum investigation reveals that carbon constitutes the majority of the elemental content of GNSC800, accounting for 98.25%. In addition to carbon, GNSC800 contains a minor quantity of oxygen, as a result of the organic composition of the groundnut shell.

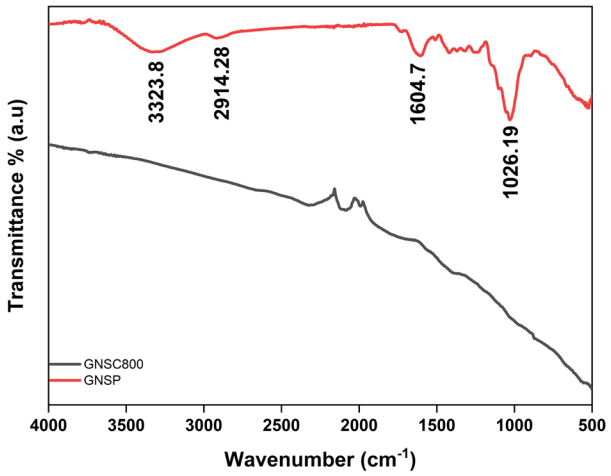

Fig. 3. FTIR spectrum of GNSP and GNSC

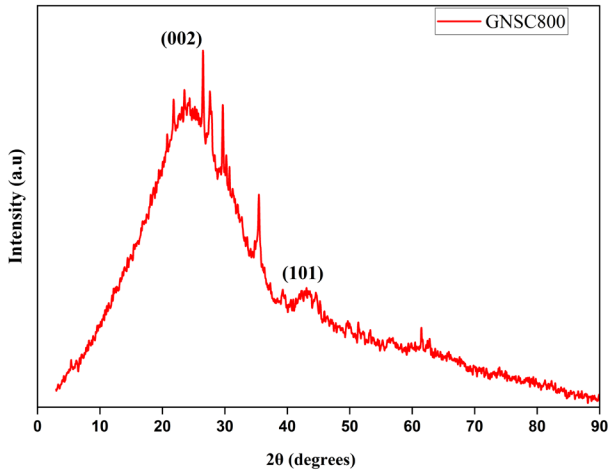

Fig. 4. XRD spectrum of GNSC800

3.2. GNSC/PLA composite characterization

3.2.1. Thermogravimetric Analysis (TGA)

The thermal characteristics of injection molded and 3D printed specimens were compared using Thermogravimetric analysis (TGA), as depicted in Fig. 6a & b. From the Fig. 6a & b it is observed the TGA curve shifted towards right hand side with the addition of GNSC nanoparticles to PLA. This indicates the improvement in thermal stability of the PLA/GNSC composites compared with neat PLA. This is also confirmed by the values of temperature at which 50% weight loss ($T_{50\,wt\%}$) occur and the

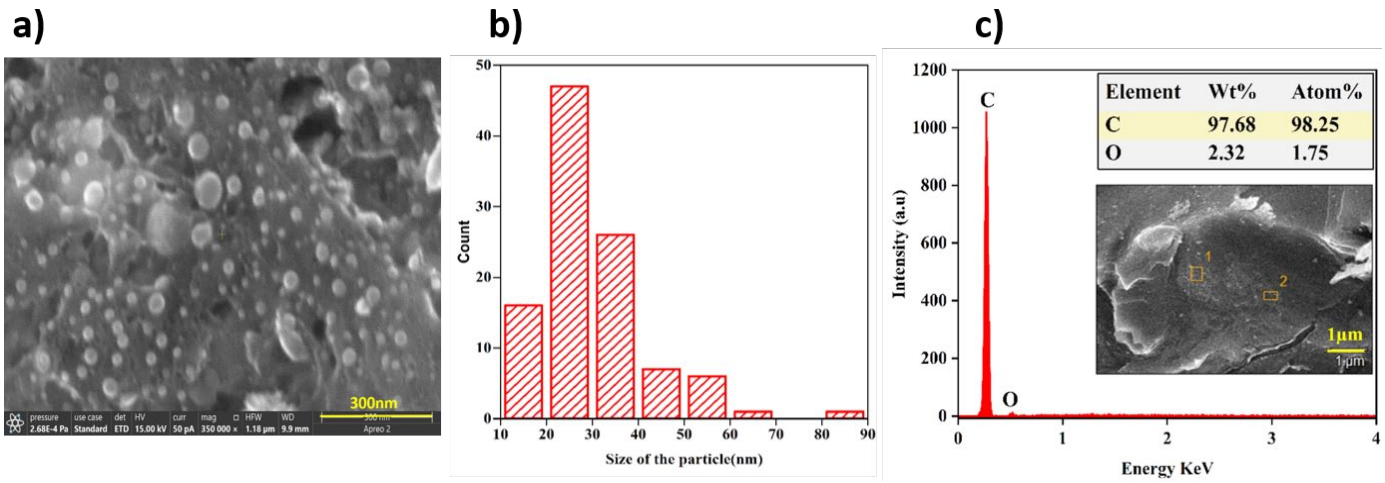

Fig. 5. a) SEM image of GNSC800 b) Histogram of carbon nanoparticles count c) EDX of GNSC800

temperature at which maximum degradation (T_{max}) occur given in TABLE 2. Regardless of the manufacturing process employed, the onset temperature, $T_{50\,wt\%}$ and T_{max} of all PLA/GNSC composites were enhanced compared to neat PLA. This improvement in thermal properties can be attributed to the uniform dispersion and strong interfacial adhesion of GNSC particles within the PLA matrix. The findings also indicate that there is no noteworthy difference in the thermal properties among injection molded and 3D printed samples. This suggests that the choice of manufacturing method does not notably impact the thermal stability of the developed composites [27]. Based on the results, it is evident that the degradation of all the samples commences at temperatures over 300°C. Therefore, the created PLA/GNSC composite material exhibits excellent thermal stability and is suitable for use in applications within the temperature range of 30-300°C, regardless of the shaping procedure employed.

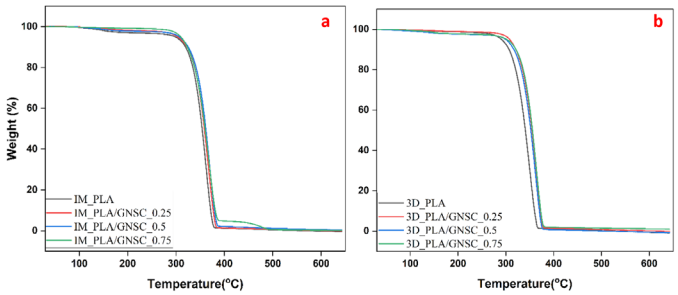

Fig. 6. a) TGA of injected molded specimen b) TGA of 3D printed samples

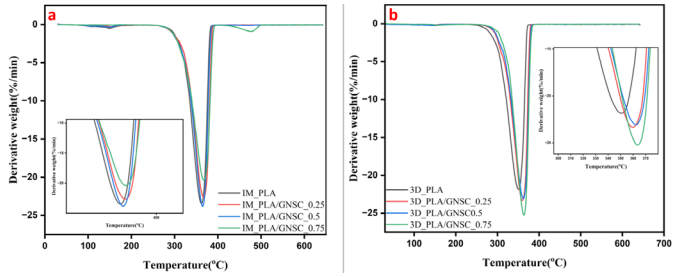

Fig. 7. a) DTG of injected molded specimen b) DTG of 3D printed specimens

TABLE 2

Comparison of thermal properties of Injected molded and 3D printed specimens

Sample code	Onset temperature (°C)	$T_{50\,wt\%}$ (°C)	T_{max} (°C)
IM_PLA	334.49	353.85	362.14
3D_PLA	316.46	340.71	350.19
IM_PLA/GNSC_0.25	337.20	358.4	367.40
3D_PLA/GNSC_0.25	330.44	354.79	359.62
IM_PLA/GNSC_0.5	344.83	359.45	369.70
3D_PLA/GNSC_0.5	343.63	352.3	362.61
IM_PLA/GNSC_0.75	339.52	356.41	367.58
3D_PLA/GNSC_0.75	331.79	354.15	362.31

3.2.2. Tensile properties

A tensile test was conducted to evaluate the strength and modulus of injection molded (IM) and 3D printed (3D) specimens. The tensile strength, modulus, and elongation percentage data obtained from the tensile test are compared in TABLE 3. The impact of the injection molding and 3D printing shaping processes on tensile properties was examined in Figs. 8 & 9. It was evident from the figure that the tensile strength and tensile modulus was improved regardless of the shaping process injection molding or 3D printing when PLA was reinforced with GNSC nanoparticles. The PLA/GNSC_0.5 exhibited the greatest tensile strength, measuring 58.61 MPa for injection molded samples and 53.05 MPa for 3D printed samples representing a 50% enhancement compared with neat PLA. Tensile modulus is calculated from the slope of the stress-strain curve using origin software. There is a little improvement in tensile modulus with the addition of GNSC particles. The PLA/GNSC_0.5 was the highest, measuring 1.24 GPa for injection molded samples and 1.21 GPa for 3D printed samples. These values reflect a 14% improvement, respectively, compared to neat PLA. The enhancement in tensile properties is due to the uniform distribution of GNSC nanoparticles which improves the interfacial adhesion between carbon nanoparticles and PLA matrix. The GNSC nanoparticles restrict the mobility of the PLA chain which enhances the tensile properties of the composite material. As the filler loading increases to 0.75%, the tensile strength and modulus start to decrease. At higher concentrations, the agglomeration behaviour of carbon nanoparticles causes a decrease in tensile strength and modulus.

TABLE 3

Comparison of tensile properties of Injected molded and 3d printed specimens

Sample code	Tensile Strength (MPa)	Tensile Modulus (GPa)	% of Strain at maximum stress
IM_Neat	39.01±1.90	1.09±0.03	5.12±0.002
3D_Neat	35.37±1.17	1.06±0.02	4.1±0.001
IM_0.25	53.39±0.72	1.17±0.04	5.80±0.001
3D_0.25	50.15±1.04	1.15±0.03	5.7±0.001
IM_0.5	58.61±1.34	1.24±0.02	6.4±0.002
3D_0.5	53.05±0.95	1.21±0.05	5.80±0.001
IM_0.75	50.48±1.46	1.12±0.06	6.02±0.004
3D_0.75	43.89±1.64	1.10±0.04	4.58±0.001

From Figs. 8 and 9 GNSC/PLA nanocomposite fabricated using the injection molding technique has higher tensile strength and modulus in comparison to those manufactured by FDM printing. Generally, the improvement in tensile properties of injection molded samples may be due to the following reasons: 1) The application of high pressures during the injection molding process enhances the bonding of polymer chains and increases the density, resulting in improved tensile properties. 2) The insufficient adhesion between the adjacent layers results in inefficient load transfer between them. 3) The temperature changes between

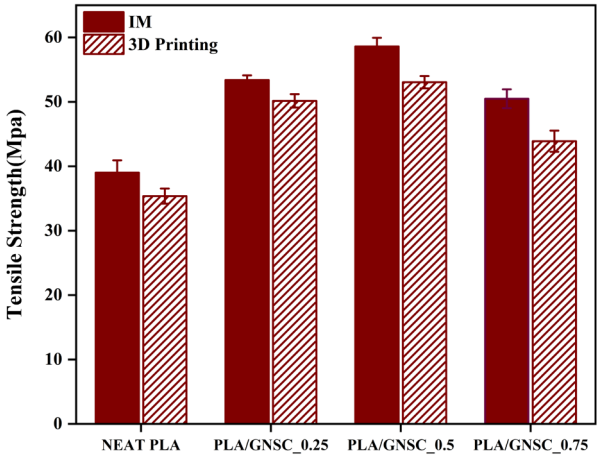

Fig. 8. Tensile strength of Injection molded and 3D printed specimens

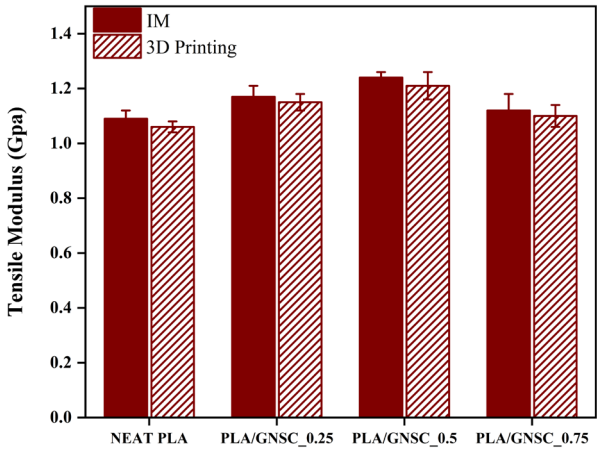

Fig. 9. Tensile modulus of Injection molded and 3D printed specimens

the adjacent layers lead to delamination which may lower the tensile properties. Nevertheless, the increase in tensile strength for injection molded and pellet 3D printing ranges from 6% to 13%, which can be considered quite modest. The increase in tensile modulus is negligible (2 to 3%). The injection molding and pellet 3D printing shaping methods have minimal influence on the tensile characteristics. This may be achieved due to the 100% infill density causing a strong bond between the layers which required a high force to break. By optimizing the process parameters, the tensile properties of the pellet 3D printing can be improved.

4. Conclusions

Carbon nanoparticles with a spherical form and a size ranging from 10 to 40nm were effectively produced by a single-step pyrolysis process employing groundnut shell powder, an agricultural waste material. The carbon nanoparticles were effectively utilized as a reinforcing filler in the fabrication of a PLA/GNSC composite. The introduction of GNSC nanoparticles improved the thermal and mechanical properties, regardless of whether the shaping technique was injection molding or pellet 3D printing. The tensile and thermal properties exhibited enhancement with increasing weight percentage of GNSC (0.25 and 0.5%). The improvement in tensile and thermal properties is due to the even distribution of carbon nanoparticles throughout the PLA matrix. The thermal and tensile properties decreased as a result of the agglomeration of carbon nanoparticles when the weight percentage of GNSC was further increased to 0.75%. The tensile strength of GNSC nanoparticles reinforced PLA composites was best for 0.5 wt% loaded samples for both injection molded and pellet 3D printed samples. The tensile strength of PLA/GNSC_0.5 was 58.61 MPa for injection molded samples and 53.05 MPa for 3D printed samples, representing a 50% enhancement compared with neat PLA. Similarly, the thermal properties, onset temperature and maximum degradation temperature were also improved with the addition of GNSC nanoparticles regardless of shaping process. The results of tensile and thermal properties revealed that there was no significant difference between injection molded and 3D printing samples. It was achieved by uniform dispersion of GNSC particles, 100% infill density and infill orientation. It can be concluded that pellet 3D printing can be effectively used by optimizing the process parameters in place of conventional injection molding.

REFERENCES

[1] K. Kumar, S. Prosenjit, S. Jaideep, Recent advances in mechanical properties of biopolymer composites: a review. 1-28 (2019). DOI: https://doi.org/10.1002/pc.25356

[2] B. Aaliya, K.V. Sunooj, M. Lackner, Biopolymer composites: a review. Int. J. Biobased Plast. **3**, 40-84 (2021). DOI: https://doi.org/10.1080/24759651.2021.1881214

[3] S. Farah, D.G. Anderson, R. Langer, Physical and mechanical properties of PLA, and their functions in widespread applications – A comprehensive review. (2016). DOI: https://doi.org/10.1016/j.addr.2016.06.012

[4] A. Bhiogade, M. Kannan, Studies on thermal and degradation kinetics of cellulose micro/nanoparticle filled polylactic acid (PLA) based nanocomposites. Polym. Polym. Compos. **29**, S85-S98 (2021). DOI: https://doi.org/10.1177/0967391120987170

[5] M. Murariu, P. Dubois, PLA composites: From production to properties. Adv. Drug Deliv. Rev. **107**, 17-46 (2016). DOI: https://doi.org/10.1016/j.addr.2016.04.003.

[6] H. Wu, W.P. Fahy, S. Kim, H. Kim, N. Zhao, L. Pilato, A. Kafi, S. Bateman, J.H. Koo, Recent developments in polymers/polymer nanocomposites for additive manufacturing. Prog. Mater. Sci. **111**, (2020). DOI: https://doi.org/10.1016/j.pmatsci.2020.100638

[7] M. Kaseem, K. Hamad, F. Deri, Y.G. Ko, A review on recent researches on polylactic acid/carbon nanotube composites. Polym. Bull. **74**, 2921-2937 (2017). DOI: https://doi.org/10.1007/s00289-016-1861-6

[8] E. Ivanov, R. Kotsilkova, H. Xia, Y. Chen, R.K. Donato, K. Donato, A.P. Godoy, R. Di Maio, C. Silvestre, S.Cimmino, V. Angelov, PLA/Graphene/MWCNT composites with improved electrical

and thermal properties suitable for FDM 3D printing applications. Appl. Sci. **9**, (2019). DOI: https://doi.org/10.3390/app9061209

[9] M.H. Omar, K.A. Razak, M.N. Ab Wahab, H.H. Hamzah, Recent progress of conductive 3D-printed electrodes based upon polymers/carbon nanomaterials using a fused deposition modelling (FDM) method as emerging electrochemical sensing devices. RSC Adv. **11**, 16557-16571 (2021). DOI: https://doi.org/10.1039/d1ra01987b

[10] C. Review, P. Malik, P. Jain, B. Reinforced, Accepted Manuscript. (2018).

[11] G. Mittal, V. Dhand, K.Y. Rhee, S.J. Park, W.R. Lee, A review on carbon nanotubes and graphene as fillers in reinforced polymer nanocomposites. J. Ind. Eng. Chem. **21**, 11-25 (2015). DOI: https://doi.org/10.1016/j.jiec.2014.03.022

[12] Y. Wu, X. Gao, J. Wu, T. Zhou, T.T. Nguyen, T. Wang, Biodegradable Polylactic Acid and Its Composites: Characteristics, Processing, and Sustainable Applications in Sports. (2023).

[13] R. Mandala, A.P. Bannoth, S. Akella, V.K. Rangari, D. Kodali, A short review on fused deposition modeling 3D printing of bio-based polymer nanocomposites. J. Appl. Polym. Sci. **139**, 1-19 (2022). DOI: https://doi.org/10.1002/app.51904

[14] R. Mandala, Development and characterization of groundnut acid composite filaments for FDM. J. Appl. Polym. Sci. 1–13 (2024). DOI: https://doi.org/10.1002/app.55689

[15] Prashant Anerao, Atul Kulkarni, Yashwanth Munde, Aninash Shinde, O. Das, Biochar reinforced PLA composite for fused deposition modelling(FDM): A parametric study on mechanical performance. Compos. Part C Open Access. (2023).

[16] E.G. Ertane, A. Dorner-Reisel, O. Baran, T. Welzel, V. Matner, S. Svoboda, Processing and Wear Behaviour of 3D Printed PLA Reinforced with Biogenic Carbon. Adv. Tribol. 2018, (2018). DOI: https://doi.org/10.1155/2018/1763182

[17] C.C. Huang, C.W. Chang, K. Jahan, T.M. Wu, Y.F. Shih, Effects of the Grapevine Biochar on the Properties of PLA Composites. Materials (Basel). **16** (2023). DOI: https://doi.org/10.3390/ma16020816

[18] A. Pudełko, P. Postawa, T. Stachowiak, K. Malińska, D. Dróżdż, Waste derived biochar as an alternative filler in biocomposites – Mechanical, thermal and morphological properties of biochar added biocomposites. J. Clean. Prod. **278** (2021). DOI: https://doi.org/10.1016/j.jclepro.2020.123850

[19] K. Aup-Ngoen, M. Noipitak, Effect of carbon-rich biochar on mechanical properties of PLA-biochar composites. Sustain. Chem. Pharm. **15**, 100204 (2020). DOI: https://doi.org/10.1016/j.scp.2019.100204

[20] C.O. Umerah, D. Kodali, S. Head, S. Jeelani, V.K. Rangari, Synthesis of carbon from waste coconutshell and their application as filler in bioplast polymer filaments for 3D printing. Compos. Part B Eng. **202**, 108428 (2020). DOI: https://doi.org/https://doi.org/10.1016/j.compositesb.2020.108428

[21] M.P. Ho, K.T. Lau, H. Wang, D. Hui, Improvement on the properties of polylactic acid (PLA) using bamboo charcoal particles. Compos. Part B Eng. **81**, 14-25 (2015). DOI: https://doi.org/10.1016/j.compositesb.2015.05.048

[22] N.B. Arzumanova, Polymer biocomposites based on agro waste: Part iii. shells of various nuts as natural filler for polymer composites. New Mater. Compd. Appl. **5**, 19-44 (2021).

[23] R. Mandala, G. Hegde, D. Kodali, V.R. Kode, From Waste to Strength: Unveiling the Mechanical Properties of Peanut-Shell-Based Polymer Composites. J. Compos. Sci. **7**, 1-22 (2023). DOI: https://doi.org/10.3390/jcs7080307

[24] M. Franchetti, C. Kress, An economic analysis comparing the cost feasibility of replacing injection molding processes with emerging additive manufacturing techniques. Int. J. Adv. Manuf. Technol. **88**, 2573-2579 (2017). DOI: https://doi.org/10.1007/s00170-016-8968-7

[25] Z. Weng, J. Wang, T. Senthil, L. Wu, Mechanical and thermal properties of ABS/montmorillonite nanocomposites for fused deposition modeling 3D printing. Mater. Des. (2016). DOI: https://doi.org/10.1016/j.matdes.2016.04.045

[26] A.T. Miller, D.L. Safranski, K.E. Smith, D.G. Sycks, R.E. Guldberg, K. Gall, Fatigue of injection molded and 3D printed polycarbonate urethane in solution. Polymer (Guildf). **108**, 121-134 (2017). DOI: https://doi.org/10.1016/j.polymer.2016.11.055

[27] C. Kaynak, S.D. Varsavas, Performance comparison of the 3D-printed and injection-molded PLA and its elastomer blend and fiber composites. J. Thermoplast. Compos. Mater. **32**, 501-520 (2019). DOI: https://doi.org/10.1177/0892705718772867

[28] U.K. Komal, B.K. Kasaudhan, I. Singh, Comparative Performance Analysis of Polylactic Acid Parts Fabricated by 3D Printing and Injection Molding. J. Mater. Eng. Perform. **30**, 6522-6528 (2021). DOI: https://doi.org/10.1007/s11665-021-05889-9

[29] M.S. Sattar, M.B. Shakoor, Comparative efficiency of peanut shell and peanut shell biochar for removal of arsenic from water. 18624-18635 (2019).

[30] L. Natrayan, S. Kaliappan, C.N. Dheeraj, K. Reddy, M. Karthick, N.S. Sivakumar, P.P. Patil, S. Sekar, S.Thanappan, Development and Characterization of Carbon-Based Adsorbents Derived from Agricultural Wastes and Their Effectiveness in Adsorption of Heavy Metals in Waste Water. 2022, (2022).

[31] M. Picard, S. Thakur, M. Misra, D.F. Mielewski, Biocarbon from peanut hulls and their green composites with biobased poly (trimethylene terephthalate) (PTT). 1-15 (2020).

[32] A.Y. Elnour, A.A. Alghyamah, H.M. Shaikh, A.M. Poulose, Effect of Pyrolysis Temperature on Biochar Microstructural Evolution, Physicochemical Characteristics, and Its Influence on Biochar / Polypropylene Composites. 7-9 (2019). DOI: https://doi.org/10.3390/app9061149